ISSN 0027-1349, Moscow University Physics Bulletin, 2010, Vol. 65, No. 5, pp. 378–385. © Allerton Press, Inc., 2010.
Original Russian Text © A.M. Lerer, 2010, published in Vestnik Moskovskogo Universiteta. Fizika, 2010, No. 5, pp. 43–49.

The Radio-Transmitting Properties of a Carbon Nanotube Vibrator Located on the Boundary of a Dielectric

A. M. Lerer

Southern Federal University, Rostov-on-Don, 344090 Russia
e-mail: lerer@sfedu.ru

Received February 24, 2010; in final form, May 7, 2010

Abstract—The quantum and mechanical properties of a carbon nanotube are described in a model with the use of a macroscopic parameter, viz., surface impedance. Solving the boundary problem for the impedance vibrator is reduced to solving paired integral equations for the vibrator current. The paired integral equations are solved by the Galerkin method with Chebyshev's basis. The influence of the substrate on the amplitude and frequency characteristics of the antenna, a carbon nanotube, is investigated.

Keywords: carbon nanotubes, nanotube-vibrator, millimeter-wave antenna, integral equations, Galerkin method.

DOI: 10.3103/S0027134910050085

INTRODUCTION

The use of carbon nanotubes (CNTs) as antennas for the centimeter and millimeter wavebands is under study. These antennas are used in communication between nanoelectronic chains and macroscopic devices. Their larger electric length in comparison to metallic vibrators has been noted [1–7], due to which resonance of the input impedance is observed in the millimeter waveband for nanotube-vibrators with a length from 20 to 50 μm. The electrical conductivity of nanotubes is highest among all known conductors with comparable sizes. The current density value that is observed at ambient temperatures in a conducting nanotube exceeds the value in superconductors by two orders of magnitude.

An idealized model, a CNT in a vacuum, has been studied in many theoretical works. This work is aimed at the development of a method for calculating and investigating the properties of CNT vibrators lying on a dielectric substrate.

The Pocklington equation with the addition of a resistive term was solved in [2–7]. With the use of the one-dimensional Green's function, this equation can be reduced to the Hallen equation. For ordinary vibrators, the more modern and accurate methods are based on integral and integro-differential equations where the source and observation points are located on the vibrator surface, in contrast to the Pocklington and Hallen equations. As a result, the integral equations have singularities, viz., logarithmic, singular, and bisingular types. These integro-differential and integral equations are typical for two-dimensional electrodynamics; therefore, there are a great number of methods for their solution. The methods that use Chebyshev's polynomials as a basis and take the Meiksner condition into account are most efficient. These methods are especially efficient with analytical regularization of integro-differential equations based on inversion of integral operators with logarithmic, singular, and bisingular kernels [8–11]. These methods can be called semi-inversion methods. One of varieties of semi-inversion methods is the application of the properties of Chebyshev's polynomials. The first- and second-type Chebyshev's polynomials are the eigen functions of integral and integro-differential operators with logarithmic kernels, respectively [12].

Methods based on collocation are competitive with these methods. Typically, these lead to systems of linear algebraic equations with a higher order than those of the above-described methods but with much simpler matrix elements, which makes the numerical implementation easier and shortens the calculation time. Since the direct application of the collocation method to integral and integro-differential equations with a kernel that has a singularity is impossible, then the initial equations are first transformed. The modified collocation method developed in [13] is essentially the Galerkin method with a basis in the form of zero-order splines. The idea of isolating a kernel with a singularity is not new (see, e.g., [14]). In [15, 16], a logarithmic singularity of the integral equation kernel was isolated and further transformations are analogous to those of the Krylov–Bogolyubov method [14]. In [17, 18], a logarithmic singularity is isolated as well. While solving the transformed integral equation, a quadrature is used that takes the rib conditions into account. In [19], unlike [17, 18], the logarithmic part of a kernel is not isolated immediately (it describes the integral equation kernel for thin vibrators poorly) but only after isolation of the static part of kernel. The

method described in [19] is applied in [20] to the calculation of CNT vibrators.

In the present work, a method of vibrator calculation is developed that is based on solving the paired integral equations with respect to the Fourier transform for the current density in a vibrator. In this case, the kernel singularity of the integro-differential equation with respect to the vibrator's current is transferred to the slow decrease of the integrand in the Fourier integral. It is easier to improve Fourier integral convergence than to regularize an integro-differential equation. For a vibration on a substrate, solving the paired integral equations is also preferable to solving integro-differential equations, because Green's function is expressed through a Fourier integral.

Let us consider a CNT that is located completely inside a dielectric with the dielectric permeability ε_1 lying on a dielectric substrate with ε_2, $\mu_1 = \mu_2 = 1$. We introduce a Cartesian coordinate system where the X axis is parallel to the substrate and perpendicular to the CNT, the Y axis is perpendicular to both the substrate and the CNT, the Z axis is directed along the vibrator, and the coordinate origin lies on the substrate. The CNT is located at $|z| \le l$ and its radius is a.

We assume that the following boundary condition is satisfied on the vibrator surface:

$$E_z = \rho_s j, \tag{1}$$

where E_z, j are the longitudinal components of the electric field strength and surface current's density, respectively; ρ_s is the CNT surface impedance [5] expressed by the formula $\rho_s = i\dfrac{\pi^2 a\hbar(\omega - i\nu)}{2e^2 v_F}$, in which v_F is the Fermi speed (for the CNT $v_F = 9.71 \times 10^5$ m/s), ω is the cyclic frequency, ν is the relaxation frequency (for the CNT $\nu = 3.33 \times 10^{11}$ Hz), e is the electron charge, c is the light speed in vacuum, and $\hbar$ is the Planck constant. The lateral component of the surface current density is neglected; j is believed to depend only on the longitudinal component.

SOLVING PAIRED INTEGRAL EQUATIONS FOR AN IMPEDANCE VIBRATOR

With the use of Green's function for the longitudinal current (see Appendix), it is easy to obtain

$$E_z(z) = \frac{1}{i\omega\varepsilon_1\varepsilon_0}\left[\frac{d^2}{dz^2}\int_{-l}^{l} j(z')g_e(z,z')dz' + k_1^2\int_{-l}^{l} j(z')g_m(z,z')dz'\right] + E_z^e(z), \tag{2}$$

where $E_z^e(z)$ is the external field. Substituting (2) into (1), we derive the integro-differential equation with respect to $j(z)$

$$\frac{1}{i\omega\varepsilon_1\varepsilon_0}\left[\frac{d^2}{dz^2}\int_{-l}^{l} j(z')g_e(z,z')dz' + k_1^2\int_{-l}^{l} j(z')g_m(z,z')dz'\right] + E_z^e(z) = \rho_s j(z), \quad |z| \le l. \tag{3}$$

At $\varepsilon_1 = \varepsilon_2$

$$g_e(z,z') = g_m(z,z') = \frac{a}{4\pi}\int_0^{2\pi}\frac{d\varphi}{R(z,z')}e^{-ikR} \approx g_0(z,z')e^{-ik|z-z'|},$$

where

$$R = \sqrt{2a^2(1-\cos\varphi) + (z-z')^2},$$

$$g_0(z,z') = \frac{a}{4\pi}\int_0^{2\pi}\frac{d\varphi}{R} = \frac{1}{2\pi}PK(P),$$

$K(P)$ is a full elliptical integral of the first type, $P = 2a/\sqrt{4a^2 + (z-z')^2}$.

In this case, as is known, an integro-differential equation is transformed to an integral equation, which is solved more easily than the initial equation. When $\varepsilon_1 \ne \varepsilon_2$, it is necessary to immediately solve integro-differential Eq. (3). While solving both integro-differential equations and integral equations, we should take into account that the Green's functions $g_{e,m}(z,z')$ have a logarithmic singularity at $z' \to z$.

Equation (3) can be transformed to the paired integral equations

$$-\frac{1}{i\omega\varepsilon_1\varepsilon_0}\frac{1}{2\pi}\int_{-\infty}^{\infty}\tilde{j}(\gamma)[\gamma^2\tilde{g}_e(\gamma) - k_1^2\tilde{g}_m(\gamma)] \times \exp(i\gamma z)d\gamma + E_z^e(z) = \rho_s j(z) \text{ at } |z| \le l,$$
$$\frac{1}{2\pi}\int_{-\infty}^{\infty}\tilde{j}(\gamma)\exp(i\gamma z)d\gamma = 0 \text{ at } |z| \ge l. \tag{4}$$

In (4) and below the symbol "~" above the function designates its Fourier transform in z.

We solve Eqs. (4) by the Galerkin method. As basis functions $V_n(z)$, we use the weighted Chebyshev's polynomials of the second kind:

$$V_n(z) = \frac{i^n}{\pi(n+1)}\sqrt{1 - \frac{z^2}{l^2}}\,U_n\left(\frac{z}{l}\right), \quad n = 0, 1, 2\ldots.$$

The Fourier transform of the polynomials $V_n(z)$ is expressed through Bessel functions: $\tilde{V}_n(\gamma) = J_{n+1}(\gamma l)/\gamma$. $\tilde{V}_n(\gamma)$ that satisfy the second equation of (4).

As a result of the solution, we derive a system of linear algebraic equations with matrix elements A_{pn} in the left-hand side and B_p in the right-hand side as follows:

$$B_p = i\omega\varepsilon_1\varepsilon_0 \int_{-l}^{l} E_z^e(z) V_p(z) dz,$$

$$A_{pn} = A_{pn}^{(1)} + A_{pn}^{(2)} + A_{pn}^{(3)},$$

where

$$A_{pn}^{(1)} = \frac{\zeta_{pn}}{\pi} \int_0^\infty (\gamma^2 - k_1^2) \tilde{g}^{(1)}(\gamma) \frac{J_{p+1}(\gamma l) J_{n+1}(\gamma l)}{\gamma^2} d\gamma, \quad (5)$$

$$A_{pn}^{(2)} = \frac{\zeta_{pn}}{\pi} \int_0^\infty (\gamma^2 \tilde{g}_e^{(2)}(\gamma) - k_1^2 \tilde{g}_m^{(2)}(\gamma)) \frac{J_{p+1}(\gamma l) J_{n+1}(\gamma l)}{\gamma^2} d\gamma,$$

$$A_{pn}^{(3)} = i\rho_s\omega\varepsilon_1\varepsilon_0 \int_{-l}^{l} V_p(z) V_n(z) dz \quad (6)$$

$$= i\rho_s\omega\varepsilon_1\varepsilon_0\zeta_{np} \frac{l}{\pi^2(p+1)(n+1)}$$

$$\times \cos\frac{q\pi}{2}\left(\frac{1}{(p+n+2)^2 - 1} - \frac{1}{(p-n)^2 - 1}\right).$$

The functions $\tilde{g}^{(1)}(\gamma)$ and $\tilde{g}_{e,m}^{(2)}(\gamma)$ are defined in Appendix; $\zeta_{pn} = 1$ if p and n are of the same parity, otherwise $\zeta_{pn} = 0$.

Integrals (5) and (6) are found numerically. We divide (5) into four integrals with ranges of integration of $[0, k_1]$, $[k_1, C]$, $[C, E]$, and $[E, \infty)$, where constants C and E are chosen from the conditions $Cl \gg \max(p, n)$, $Ea \gg 1$. In the first integral, we make the substitution of variables $\gamma = k_1\cos\psi$; in the second integral, $\gamma = k_1\cosh\theta$. Both integrals are then calculated by the rectangular formula. In the third integral, we substitute the Bessel functions for their asymptotic $J_{p+1}(\gamma l)J_{n+1}(\gamma l) \approx \frac{1}{\pi\gamma l}\cos\left(\frac{p-n}{2}\pi\right)$, the transformed integral is calculated by the rectangular formula. In the fourth integral we substitute the Bessel functions and $\tilde{g}^{(1)}(\gamma)$ for their asymptotics; the transformed integral is found analytically. Thus, the slow decrease (such as γ^{-2} at $\gamma \to \infty$) of the integrand of (5) is taken into consideration.

Integral (6) is a double integral. We transfer to the new variables $\alpha = \rho\cos\theta$, $\gamma = \rho\sin\theta$. The integral with respect to θ is calculated by the rectangular formula. In the integral with respect to ρ, the integration is performed only over the intervals $[0, k_1]$ and $[k_1, C]$. We calculate these integrals in the same manner as the appropriate integrals with respect to γ in (5).

NUMERICAL RESULTS

A C++ program was created. The kernels of integrals (5) and (6) are the same for all matrix elements. They are calculated once and stored as $\tilde{V}_n(\gamma)$. This reduces the computation time by an order of magnitude. The run time for one point on the frequency characteristics using a personal computer (the processor's clock rate is 2.33 GHz) is 0.4 s for a CNT on a substrate and 0.015 s for a CNT without a substrate, which is less by an order than the time of computation using the modified collocation method for the CNT without a substrate. Two variants of the external field are used: the incidence of the plane electromagnetic wave and excitation from the delta-shaped source $E_z^e(z) = \delta(z)$. Further, the results for the second variant are given. The nanotube length $2l = 20$ μm.

The study of the input impedance Z_{in} of the isolated single-layer CNT vibrators was performed. The input impedance normalized to $R_0 = h/(2e^2) \approx 12.9$ kΩ is given in Figs. 1–3. The dotted curves present the imaginary part of Z_{in}.

Investigations of the internal convergence of the solution were conducted. The number of basis functions (the order of the system of linear algebraic equations) M becomes greater, naturally, when the electrical length of the CNT increases and ε_1, ε_2 grows. For Z_{in} computations with an error in the internal convergence of less than 1% at $f = 250$ GHz (the vibrator is fitted by the half length of the plasma wave propagating along the CNT), it is sufficient to assume $M = 10$; at $f = 1000$ GHz (eight half-waves), $M = 50$. The rate of the internal convergence of the computations of the far field with any means of excitation is 3–5 times greater than that in the Z_{in} computation.

The frequency characteristics of nanotube vibrators located on the substrate surface (curve *1*) are plotted in Figs. 1 and 2. Their Z_{in} values differ drastically from Z_{in} values without account for the substrate (curve *3*); at low frequencies and small ε they approach the Z_{in} values for a vibrator placed inside a homogeneous dielectric with ε equal to the arithmetic mean of ε values for the substrate and vacuum (curve *2*). As the frequency grows, the field is drawn deeper inside the dielectric and the distinction between curves *3* and *2* increases. The resonant frequencies grow as radius a is reduced. Figure 1 also shows the plot of the imaginary part of Z_{in} for a perfectly conducting metallic vibrator on the substrate (curve *4*). The real part $Z_{\text{in}} \ll R_0$. It should be noted that a perfectly conducting metallic vibrator with analogous sizes has a first resonant frequency that equals approximately 7.255 THz for the vibrator in air and 6.0 THz for the vibrator on a substrate with $\varepsilon_2 = 2.2$.

Figure 3 illustrates the frequency characteristic of a nanotube-vibrator embedded in the substrate (curve *2*). At low frequencies, its Z_{in} values approach the Z_{in} values of a vibrator placed inside a homogeneous dielec-

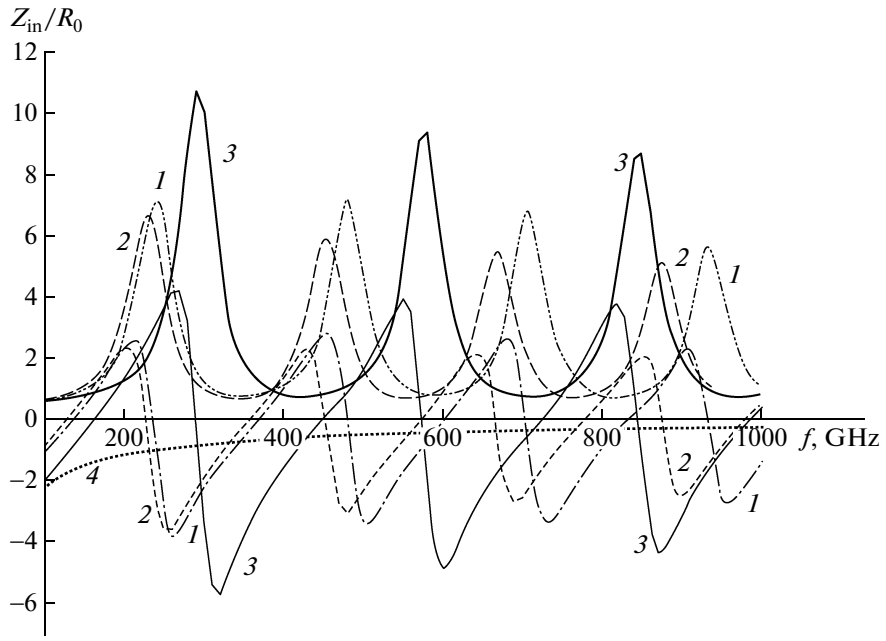

Fig. 1. Dependence of a nanotube's input impedance on frequency. The nanotube is located on the surface of a substrate with $\varepsilon_2 = 2.2$, radius $a = 2.712$ nm. The curves correspond to the cases of $\varepsilon_1 = 1$ and $\varepsilon_2 = 2.2$ (curve *1*); $\varepsilon_1 = \varepsilon_2 = 1.6$ (curve *2*); $\varepsilon_1 = \varepsilon_2 = 1$ (curve *3*), and a perfectly conducting vibrator (curve *4*).

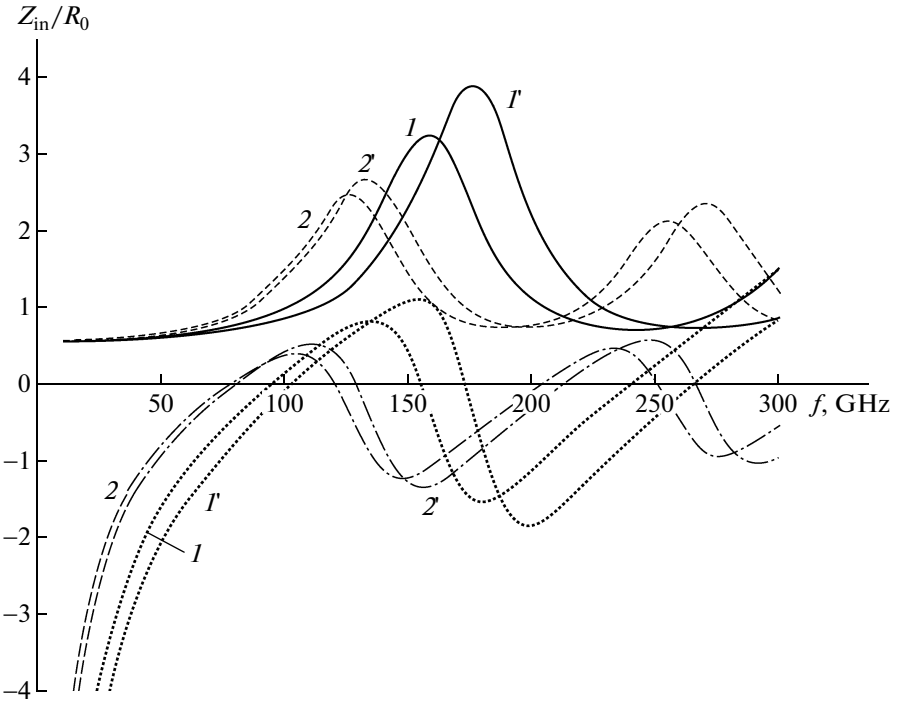

Fig. 2. Dependence of a nanotube's input impedance on frequency. The nanotube is located on the surface of a substrate with $\varepsilon_2 = 9$. Curves *1* and *1*' correspond to $\varepsilon_1 = 1$ and $\varepsilon_2 = 9$; curves *2* and *2*', to $\varepsilon_1 = \varepsilon_2 = 5$. Radius $a = 2.712$ nm (curves *1* and *2*) and 1.356 nm (curves *1*' and *2*').

tric with a dielectric permeability equal to that of the substrate (curve *1*).

The amplitude–frequency dependences of the far field have extremums at points where the imaginary part of the input impedance becomes zero. In this case the maximums (minimums) of the electric field strength correspond to the minimums (maximums) of the real part of the input impedance.

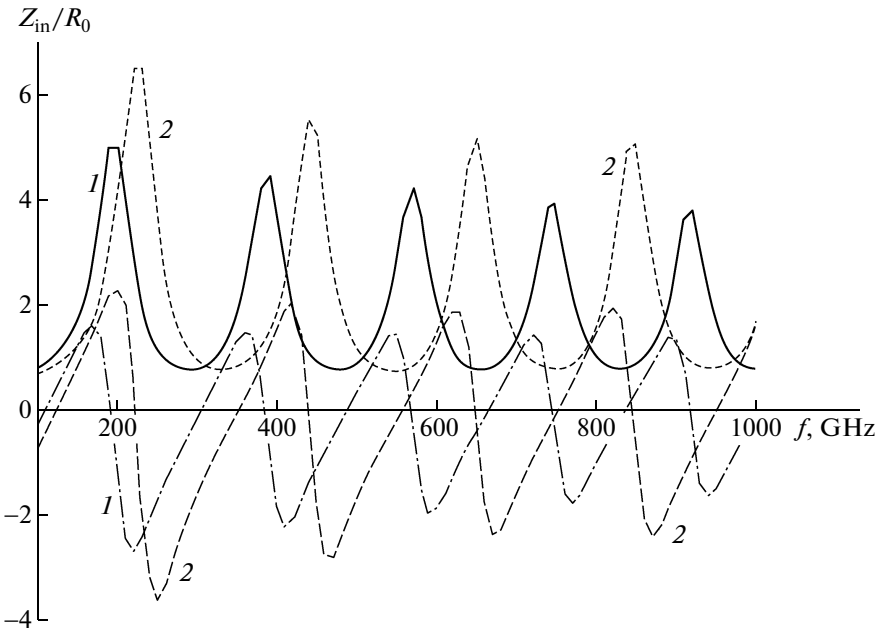

Fig. 3. Dependence of a nanotube's input impedance on frequency. The nanotube is embedded in a substrate, radius a = 2.712 nm. Curve *1* corresponds to $\varepsilon_1 = \varepsilon_2 = 2.2$; curve *2*, to $\varepsilon_1 = 2.2$, $\varepsilon_2 = 1$.

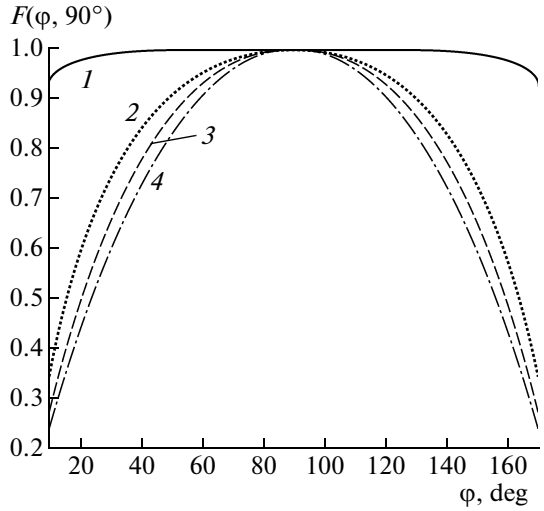

Fig. 4. Directivity diagram of a nanotube on a substrate (*H* plane; $\varepsilon_1 = 1$; $\varepsilon_2 = 1.01$ (curve *1*), 2.2 (curve *2*), 4 (curve *3*), and 9 (curve *4*)).

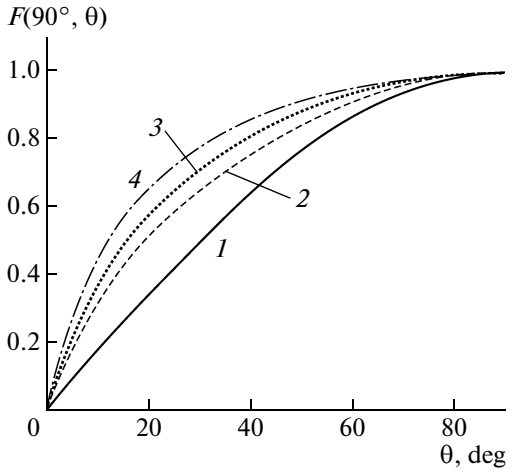

Fig. 5. Directivity diagram of a nanotube on a substrate (*E* plane; the ε values and designations of curves are the same as in Fig. 4).

Figures 4 and 5 present the directivity diagrams $F(\varphi, \theta)$ in the upper half plane. The φ angle is counted from the substrate and the θ angle is counted from the vibrator. The frequency f = 100 GHz. As the substrate's dielectric permeability ε_2 increases, the directivity diagram in the *H* plane (perpendicular to the nanovibrator and passing through its center) contracts, but in the *E* plane (passing through the nanovibrator) it expands. The upward-radiation power grows as ε_2 increases.

CONCLUSIONS

The solution of the boundary problem on the excitation of a CNT vibrator is reduced to solving paired integral equations. It is preferable to use paired integral equations rather than integro-differential equations because the Green's function of the problem is expressed through the Fourier integral. The quantum and mechanical properties of the carbon nanotube are described in the model with the use of a macroscopic parameter, viz., surface impedance. The paired inte-

gral equations were solved by the Galerkin method. During the solution of the paired integral equations, the singularity of the integral equation kernel was manifested in the slow convergence of integrals in matrix elements of the derived linear algebraic equations. The convergence of these integrals was improved. The fast internal convergence of the solution was shown. The influence of the substrate on the amplitude–frequency characteristics of the antenna, a carbon nanotube, was investigated. It was shown that these characteristics can be described with the introduction of efficient dielectric permeability $\varepsilon_{\text{eff}} = (\varepsilon_1 + \varepsilon_2)/2$ only at low frequencies and small values of the substrate dielectric permeability.

APPENDIX

THE GREEN'S FUNCTION FOR VIBRATOR

Let us define the electromagnetic field created by the longitudinal current $j_z\delta(x-x')\delta(y-y')\delta(z-z')$ as the superposition of *LM* and *LE* waves described by the y components of the electric and magnetic vector potentials $A(x, x', y, y', z, z')$ and $F(x, x', y, y', z, z')$ [21]. It is assumed that $y' \geq 0$. We designate the Fourier transform of A and F by coordinates as $\tilde{A}(y, y', \alpha, \gamma)\exp[-i(\alpha x' + \gamma z')]$ and $\tilde{F}(y, y', \alpha, \gamma)\exp[-i(\alpha x' + \gamma z')]$. Functions A and F are solutions to the differential equations

$$\left(\frac{\partial^2}{\partial y^2} + \beta_j^2\right)\begin{Bmatrix}\tilde{A}(y, y', \alpha, \gamma)\\ \tilde{F}(y, y', \alpha, \gamma)\end{Bmatrix} = 0, \tag{A.1}$$

where $\beta_j = \sqrt{\rho^2 - k_j^2}$, $\rho^2 = \alpha^2 + \gamma^2$, $k_j = k\sqrt{\varepsilon_j}$, k is the wavenumber in vacuum. Equations (A.1) are valid at $y \neq y'$. We seek the solution in the form

$$\begin{aligned}\tilde{A}(y, y', \alpha, \gamma) &= i\omega\varepsilon_1\varepsilon_0 a(\alpha, \gamma) U_e(y, y', \alpha, \gamma),\\ \tilde{F}(y, y', \alpha, \gamma) &= b(\alpha, \gamma) U_m(y, y', \alpha, \gamma),\end{aligned} \tag{A.2}$$

where $a(\alpha, \gamma)$ and $b(\alpha, \gamma)$ are the unknown coefficients and

$$U_e(y, y', \alpha, \gamma) = \begin{cases} M^-(y, \alpha, \gamma)M'^+(y', \alpha, \gamma), & y \leq y'\\ M^+(y, \alpha, \gamma)M'^-(y', \alpha, \gamma), & y \geq y',\end{cases}$$

$$U_m(y, y', \alpha, \gamma) = \begin{cases} E^-(y, \alpha, \gamma)E^+(y', \alpha, \gamma), & y \leq y'\\ E^+(y, \alpha, \gamma)E^-(y', \alpha, \gamma), & y \geq y';\end{cases}$$

indices "±" designate the solutions respectively at $y \geq y'$, $y \leq y'$; $M'^{\pm}(y, \alpha, \gamma) = \frac{\partial}{\partial y} M^{\pm}(y, \alpha, \gamma)$; $M^{\pm}(y, \alpha, \gamma)$ and $E^{\pm}(y, \alpha, \gamma)$ in every layer satisfy Eq. (A.1) and the radiation condition. At the interface of dielectrics, the following functions are continuous:

$$\begin{aligned}&M^{\pm}(y, y', \alpha, \gamma), \quad E^{\pm}(y, y', \alpha, \gamma),\\ &\frac{1}{\varepsilon}\frac{\partial}{\partial y}M^{\pm}(y, y', \alpha, \gamma), \quad \frac{1}{\mu}\frac{\partial}{\partial y}E^{\pm}(y, y', \alpha, \gamma).\end{aligned} \tag{A.3}$$

Condition (A.3) of continuity of functions is a consequence of continuity conditions of tangential components of the intensities of electric and magnetic fields. From (A.2) is seen the continuity of the functions $\frac{\partial}{\partial y}\tilde{A}(y, y', \alpha, \gamma)$ and $\tilde{F}(y, y', \alpha, \gamma)$ at $y = y'$. This means that $E_{x,z}$ will be continuous at $y = y'$.

Using (A.2), we find the Fourier transform of all components of the electromagnetic field. We express the unknowns $a(\alpha, \gamma)$ and $b(\alpha, \gamma)$ through the longitudinal component of the current density j_z

$$\begin{aligned}\mp j_{z,x} &= \tilde{H}_{x,z}(y' + 0, y', \alpha, \gamma) - \tilde{H}_{x,z}(y' - 0, y', \alpha, \gamma)\\ &= -\omega\varepsilon_1\varepsilon_0 a(\alpha, \gamma)\varphi_e(\alpha, \gamma)\begin{Bmatrix}\gamma\\ -\alpha\end{Bmatrix}\\ &\quad - \frac{1}{\omega\mu_0} b(\alpha, \gamma)\varphi_m(\alpha, \gamma)\begin{Bmatrix}\alpha\\ \gamma\end{Bmatrix},\end{aligned} \tag{A.4}$$

where

$$\begin{aligned}\varphi_e(\alpha, \gamma) &= M^-(y', \alpha, \gamma)M'^+(y', \alpha, \gamma)\\ &\quad - M^+(y', \alpha, \gamma)M'^-(y', \alpha, \gamma),\\ \varphi_m(\alpha, \gamma) &= E'^-(y', \alpha, \gamma)E^+(y', \alpha, \gamma)\\ &\quad - E'^+(y', \alpha, \gamma)E^-(y', \alpha, \gamma).\end{aligned}$$

As $j_x = 0$, so from (A.4) we derive

$$\begin{aligned}a(\alpha, \gamma) &= \frac{Z_{c1}}{k_1}\frac{\gamma}{\rho^2\varphi_e(\alpha, \gamma)} j_z,\\ b(\alpha, \gamma) &= Z_{c1}\frac{\alpha k_1}{\rho^2\varphi_m(\alpha, \gamma)} j_z,\end{aligned} \tag{A.5}$$

where $Z_{c1} = \sqrt{\mu_0/(\varepsilon_1\varepsilon_0)}$.

Now we find the expression for $E_z(y, y', \alpha, \gamma)$ and substitute (A.5) in it. As a result, we obtain

$$\begin{aligned}&E_z(y, y', \alpha, \gamma)\\ &= i\frac{k_1}{Z_{c1}\rho^2}\left[\frac{\gamma^2}{\varphi_e(\alpha, \gamma)} U'_e(y, y', \alpha, \gamma)\right.\\ &\quad \left. - \frac{\alpha^2 k_1^2}{\varphi_m(\alpha, \gamma)} U_m(y, y', \alpha, \gamma)\right]\\ &= i\frac{k_1}{Z_{c1}}[\gamma^2\tilde{G}_e(y, y', \alpha, \gamma) - k_1^2\tilde{G}_m(y, y', \alpha, \gamma)],\end{aligned}$$

where

$$\tilde{G}_e(y, y', \alpha, \gamma) = \frac{1}{\rho^2}\left[\frac{U_e'(y, y', \alpha, \gamma)}{\varphi_e(\alpha, \gamma)} + \frac{k_1^2 U_m(y, y', \alpha, \gamma)}{\varphi_m(\alpha, \gamma)}\right],$$

$$\tilde{G}_m(y, y', \alpha, \gamma) = \frac{U_m(y, y', \alpha, \gamma)}{\varphi_m(\alpha, \gamma)}.$$

The derived formulas are valid for any dielectric with flat interface boundaries between dielectrics. For a two-layer dielectric (see Fig. 1), it is easy to obtain

$$M^+(y, \alpha, \gamma) = E^+(y, \alpha, \gamma) = \exp(-\beta_1 y), \quad y \geq y',$$

$$M^-(y, \alpha, \gamma) = \begin{cases} \varepsilon_1[\varepsilon_2\beta_1\cosh(\beta_1 y) + \varepsilon_1\beta_2\sinh(\beta_1 y)], & y' \geq y \geq 0 \\ \varepsilon_1\varepsilon_2\beta_1\exp(\beta_2 y), & y \leq 0, \end{cases}$$

$$E^-(y, \alpha, \gamma) = \begin{cases} \beta_1\cosh(\beta_1 y) + \beta_2\sinh(\beta_1 y), & y' \geq y \geq 0 \\ \beta_1\exp(\beta_2 y), & y \leq 0, \end{cases} \quad \text{(A.6)}$$

$$\tilde{G}_{e,m}(y, y', \alpha, \gamma) = \frac{1}{2\beta_1} \times \{\exp[-\beta_1|y - y'|] + R_{e,m}(\alpha, \gamma)\exp[-\beta_1(y + y')]\},$$

where

$$R_e(\alpha, \gamma) = (\varepsilon_1 - \varepsilon_2)\frac{\beta_1(\beta_1 + \beta_2) - k_1^2}{(\beta_1 + \beta_2)(\varepsilon_2\beta_1 + \varepsilon_1\beta_2)},$$

$$R_m(\alpha, \gamma) = \frac{\beta_1 - \beta_2}{\beta_1 + \beta_2}.$$

At $\varepsilon_1 = \varepsilon_2$, we have $R_{e,m} = 0$.

Although the inverse Fourier transform of the first term from (A.6) in α and γ can be found analytically (this is the well-known three-dimensional Green's function for the dielectric with the dielectric permeability ε_1), we shall use its integral representation.

Now let us find the Fourier transforms of the Green's function, which enter the paired integral Eqs. (4). We convert to variables $x = a\cos\varphi$, $y = a + a\sin\varphi$, $x' = a\cos\varphi'$, $y' = a + a\sin\varphi'$:

$$\tilde{g}_{e,m}(\gamma) = \frac{a}{(2\pi)^2}\int_0^{2\pi} d\varphi \int_0^{2\pi} d\varphi' \times \int_{-\infty}^{\infty} \tilde{G}_{e,m}(y, y', \alpha, \gamma)\exp[i\alpha(x - x')]d\alpha$$

$$= a\left[I_0(\eta a)K_0(\eta a) + \int_0^{\infty} R_{e,m}(\alpha, \gamma)I_0^2(\eta a)\frac{\exp(-2\beta_1 a)}{\beta_1}d\alpha\right] = \tilde{g}^{(1)}(\gamma) + \tilde{g}^{(2)}_{e,m}(\gamma),$$

where $I_0(\eta a)$, $K_0(\eta a)$ are modified Bessel functions, $\eta = \sqrt{\gamma^2 - k_1^2}$.

In (2) and (3) the functions

$$g_{e,m}(z, z') = \frac{1}{2\pi}\tilde{g}_{e,m}(\gamma)\exp[i\gamma(z - z')]d\gamma$$

enter.

ACKNOWLEDGMENTS

The work was supported by the Russian Foundation for Basic Research, grant no. 09-02-13530ophi_ts.

REFERENCES

1. P. J. Burke, Shengdong Li, and Zhen Yu, IEEE Trans. Nanotecnol. **5**, 314 (2006).
2. G. W. Hanson, IEEE Trans. Antennas Propagat. **53**, 3426 (2005).
3. G. W. Hanson, IEEE Trans. Antennas and Propagation **53** (11), 3426 (2005).
4. J. Hao and G. W. Hanson, IEEE Trans. Nanotechnol. **5**, 766 (2006).
5. M. V. Shuba, G. Ya. Slepyan, and S. A. Maksimenko, Phys. Rev. **79**, 155403 (2009).
6. A. M. Attiya, in *Proc. of the Conf. on Progress in Electromagnetics Research, PIERS 94* (2009), p. 419.
7. G. W. Hanson, IEEE Antennas Propagat. Mag. **50** (3), 66 (2008).
8. E. A. Gusseinov and A. S. Il'inskii, Zh. Vychisl. Mat. Mat. Fiz. **27**, 1050 (1987).
9. I. K. Lifanov and A. S. Nenashev, Elektromagn. Volny Elektron. Sist. **8** (5), 25 (2003).
10. S. I. Eminov, Radiotekh. Elektron. **38**, 2161 (1993).
11. V. A. Neganov, D. P. Tabakov, and G. P. Yarovoi, *Modern Theory and Practical Applications of Antennas* (Moscow, 2009) [in Russian].
12. A. B. Kleshchenkov, A. M. Lerer, and O. S. Labun'ko, Usp. Sovrem. Radioelektron., No. 6, 60 (2006).
13. S. I. Eminov, Pis'ma Zh. Tekh. Fiz. **31** (15), 55 (2005) [Tech. Phys. Lett. **31**, 656 (2005)].

14. L. V. Kantorovich and V. I. Krylov, *Approximate Methods of Higher Analysis* (Gostekhizdat, Moscow, 1950; Wiley, New York, 1964).

15. W. Pearson, IEEE Trans. Antennas Propagat. **23**, 256 (1975).

16. C. M. Butler, IEEE Trans. Antennas Propagat. **23**, 293 (1975).

17. A. M. Lerer and A. A. Yachmenov, Radiotekh. Elektron. **49**, 445 (2004) [J. Commun. Technol. Electron. **49**, 411 (2004)].

18. A. M. Lerer, V. V. Makhno, and A. A. Yachmenov, Radiotekh. Elektron. **51**, 46 (2006) [J. Commun. Technol. Electron. **51**, 40 (2006)].

19. A. M. Lerer, A. B. Kleshchenkov, V. A. Lerer, et al., Radiotekh. Elektron. **53**, 423 (2008) [J. Commun. Technol. Electron. **53**, 397 (2008)].

20. A. M. Lerer, V. V. Makhno, P. V. Makhno, and G. A. Shurov, Elektromagn. Volny Elektron. Sist., No. 3, 15 (2010).

21. Yu. V. Egorov, *Partially Filled Rectangular Waveguides* (Sov. Radio, Moscow, 1967) [in Russian].